Application of Volumetric Modulated Arc Therapy and Simultaneous Integrated Boost Techniques to Prepare "Safe Margin" in the Rabbit VX2 Limb Tumor Model

Authors' Contribution:
Study Design **A**
Data Collection **B**
Statistical Analysis **C**
Data Interpretation **D**
Manuscript Preparation **E**
Literature Search **F**
Funds Collection **G**

ABCDEF 1 **Chong-Wen Wang**
B 1 **Yang Zhou**
AG 1 **Jing-Ping Bai**
E 2 **Hao Liu**
D 3 **Yan Liu**
B 1 **Guang-Li Shi**
D 4 **Jiao-Jiao Ding**
E 2 **Dong-Hui Ma**
D 5 **Wen-Ting Li**
C 1 **Peng-Ming Xie**
B 1 **Yue Yan**

1 Department of Bone and Soft Tissue, The Affiliated Tumor Hospital of Xinjiang Medical University, Urumqi, Xinjiang, P.R. China
2 Department of Radiotherapy, The Affiliated Tumor Hospital of Xinjiang Medical University, Urumqi, Xinjiang, P.R. China
3 Department of Magnetic Resonance Imaging, The Affiliated Tumor Hospital of Xinjiang Medical University, Urumqi, Xinjiang, P.R. China
4 Department of Ultrasound, The First Affiliated Hospital of Xinjiang Medical University, Urumqi, Xinjiang, P.R. China
5 Department of Pathology, The Affiliated Tumor Hospital of Xinjiang Medical University, Urumqi, Xinjiang, P.R. China

Corresponding Author: Jing-Ping Bai, e-mail: xjbaijingping@sina.com
Source of support: This experiment was supported by the Xinjiang Uygur Autonomous Region Graduate Innovation Foundation (XJGRI2014090) and Xinjiang Uygur Autonomous Region Natural Science Foundation (2015211C114)

Background: In this study, we aimed to establish the rabbit VX2 limb tumor model, and then prepare a "necrotic zone" as a safe margin by volumetric modulated arc therapy and simultaneous integrated boost (VMAT-SIB) technique applied in the areas where the tumor is located adjacent to the bone (GTV_{boost} area).

Material/Methods: Rabbits in the control group (n=10) were not treated, while those in the test group (n=10) were treated with the SIB schedule delivering a dose of 40Gy, 35Gy, 30Gy, and 25Gy to the GTV_{boost}, GTV (gross tumor volume), CTV (clinical target volume), and PTV (planning target volume) in 10 fractions. Magnetic resonance diffusion-weighted imaging (MRDWI), 3-dimensional power Doppler angiography (3D-PDA), and histological changes were observed after radiotherapy.

Results: After radiotherapy, the two groups showed a significant difference in the GTV_{boost} area. In the test group, the tumor necrosis showed a significantly low signal in DWI and high signal in apparent diffusion coefficient (ADC) maps. The 3D-PDA observation showed that tumor vascular structures decreased significantly. Histological analysis demonstrated that a necrotic zone could be generated in the GTV_{boost} area, and microscopic examination observed cell necrosis and fibroplasia.

Conclusions: This studies demonstrated the feasibility of using VMAT-SIB technique in the rabbit VX2 limb tumor model. The formation of a necrotic zone can be effectively defined as safe margin in the GTV_{boost} area. showing potential clinical applicability.

MeSH Keywords: Rabbits • Radiotherapy, Intensity-Modulated • Diffusion Magnetic Resonance Imaging • Ultrasonography, Doppler • Histological Techniques

Full-text PDF: http://www.medscimonit.com/abstract/index/idArt/894909

📄 3560   ▦ 1   📊 6   📑 28

Background

Soft tissue sarcoma (STS) occurs most frequently in the extremities [1]. In most cases, the treatment involves surgical excision of the tumor. The goal of surgery is to achieve tumor resection with a wide margin (2 to 3 cm) whenever possible, removing at least one uninvolved tissue plane circumferentially [2]. In case of high-grade limb STS with tumor invasion in neurovascular bundle (NVB) or bones, wide resection is difficult because of the need for preservation of the limb. However, this may result in positive surgical margins that have a higher chance of local recurrence rate [1,3,4]. Currently, limb-sparing surgery combined with adjuvant radiotherapy is the primary treatment for high-grade limb STS. This improves local control and quality-of-life in patients [5–7]. Previous studies confirmed that preoperative radiotherapy is superior to postoperative radiotherapy [8,9].

Recently, volumetric modulated arc therapy and simultaneous integrated boost (VMAT-SIB) technique has been adopted in treating tumors at different sites [10–12]. VMAT permits the delivery of highly conformal dose distributions. It can be delivered in less than 3 min, achieving excellent target coverage and normal tissue sparing with acceptable acute toxicity [10–12]. Using SIB technique, multiple target volumes receiving different prescribed doses can be integrated into a single treatment plan [13].Previous studies has shown that implementation of radiotherapy in the rabbit VX2 tumor model is feasible, and radiation can cause tumor necrosis[14].However, still is not reported, if the rabbit VX2 tumor model can implement VMAT-SIB technique.

Based on our imaging studies of tumors resected from high-grade limb STS cases, we found that some tumors did not invade the NVB or bone, but were located adjacent to these structures (Figure 1A). Thus, we hypothesized that STS is an irregularly shaped solid tumor with one surface or an edge adjacent to the NVB or bones. Using VMAT-SIB, we could increase the radiation dose in the areas where the tumor is located adjacent to the bone (i.e., when the delineated the target volume is defined as GTV_{boost} area) (Figure 1B). This enhances

local tissue injury and a necrotic zone could be generated (i.e., macroscopic and microscopic observed the cell necrosis in the GTV_{boost} area).We defined such necrotic zone as "safe margin".

The aim of this study was to establish the rabbit VX2 limb tumor model, and then prepare a necrotic zone as safe margin by a VMAT-SIB technique applied in the GTV_{boost} area. Using Magnetic resonance diffusion-weighted imaging (MRDWI), three-dimensional power Doppler angiography (3D-PDA) and histological change, the feasibility and effectiveness of the prepared safe margin would be evaluated.

Material and Methods

Ethics statement

This study was approved by the ethics committee of the First Affiliated Hospital of Xinjiang Medical University, China (Approval No. IACUC20131105007). The animal research platform was certified by the Association for Assessment and Accreditation of Laboratory Animal Care (AAALAC).

Animals and establishment of the VX2 limb tumor model

Twenty-six healthy male New Zealand white rabbits were included in this study. They weighted 3.5 to 4.0 kg and aged 6 to 8 months. The animals were provided by the Experimental Animal Center of Xinjiang Medical University (use permit: SYXK2010-0002). The donor animals (n=6) were used to propagate the VX2 tumor cells. Anesthesia was provided using intramuscular injection of 3% pentobarbital sodium (Alvetra, Neumuenster, Germany) at a dose of 1.5 ml/kg. VX2 solid tumor (Guangzhou Jennio Biotech Co. Ltd., Guangdong, China) was implanted in the left hind limb muscle of tumor-bearing rabbits. Two weeks later, the solid tumor was harvested and minced to tissue pieces of approximately 0.5×0.5 mm in a clean bench to prepare a tumor suspension. This suspension was then implanted in the study animals under general anesthesia following aseptic and antiseptic precautions. B-Ultrasound guided (LOGIQ E9; GE
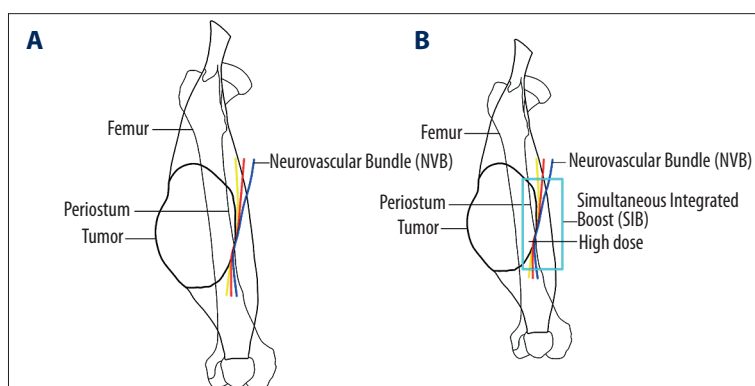

Figure 1. (**A**) Tumor adjacent to the NVB and bone. (**B**) Enhancing radiation at GTV_{boost} area using SIB.

Labels in Figure 1A: Femur; Neurovascular Bundle (NVB); Periostum; Tumor

Labels in Figure 1B: Femur; Neurovascular Bundle (NVB); Periostum; Tumor; Simultaneous Integrated Boost (SIB); High dose
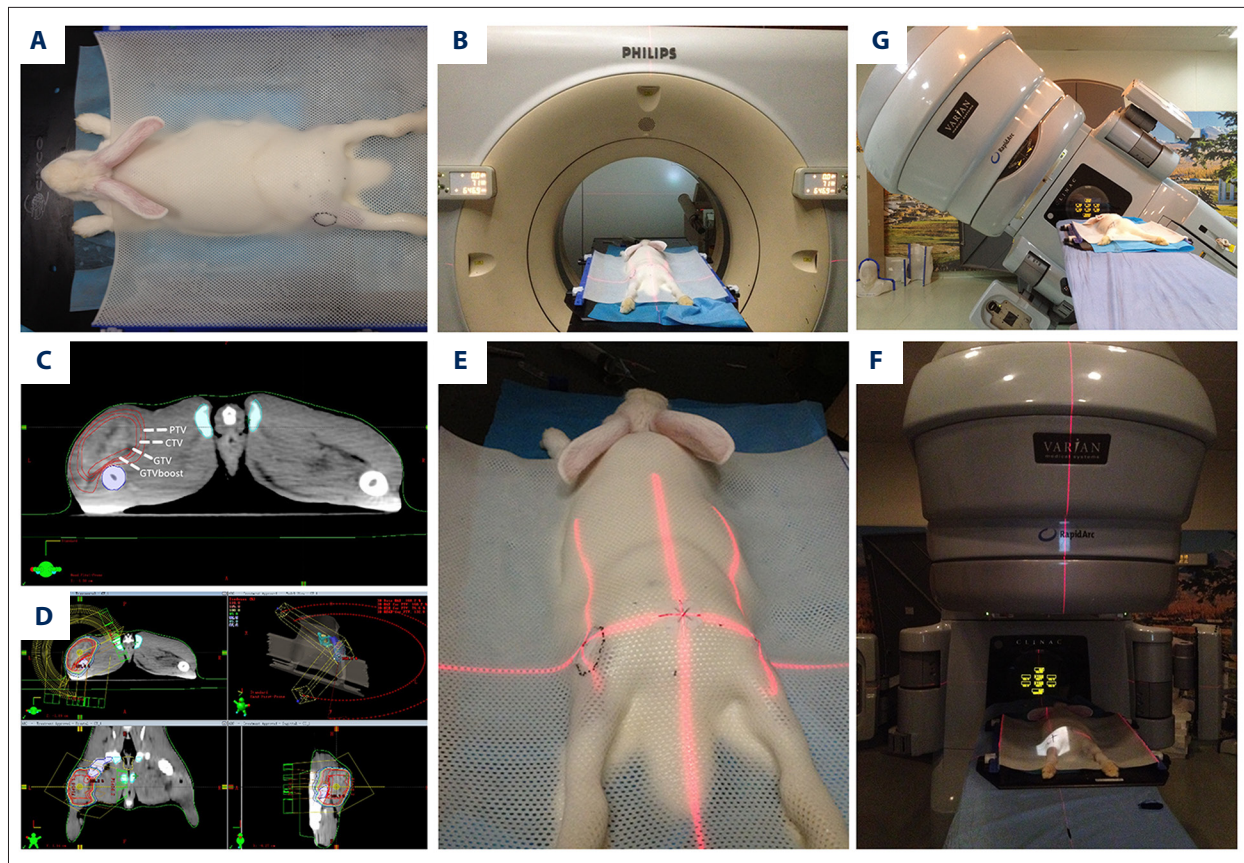
Figure 2. Radiotherapy process. (**A**) Making thermoplastic; (**B**) Localization using Big Bore CT simulation scan; (**C**) delineation of the target volumes; (**D**) using two full arcs, (**E**) center calibration after the plan has been completed; (**F**) position restoration before radiotherapy; (**G**) radiotherapy.

Healthcare, Milwaukee, WI, USA) tumor implantation was performed by injecting 0.5 ml of tumor suspension using a 14-G needle into the left hind limb muscle (adjacent to the bone). Tumor growth was monitored using a diagnostic ultrasound device (LOGIQ E9; GE Healthcare, Milwaukee, WI, USA). After 12 days, solid tumor (size 3.0–3.5 cm) was detected by ultrasound in the left hind limb of 20 animals. The limited tumor size range (3.0–3.5 cm) and the fixed growth site (adjacent to the bone) were controlled during the establishment of the tumor model for the following comparable study.

Experimental protocol

The VX2 tumor was implanted in a total of 20 animals, which were then randomly divided into the control group (untreated, n=10) and the test group (radiotherapy, n=10). The test group received radiotherapy 2 weeks after tumor implantation. The imaging of the 2 groups was collected on the 7 days after radiotherapy. The histological changes were observed after sacrificing the animals with over-dose of pentobarbital euthanasia. During each imaging and radiotherapy, test group were anesthetized, while the control group only received anesthesia at

the time of image acquisition. At the end of anesthesia, animals were given low-flow oxygen (10 min) and saline infusion (marginal ear vein, 40 ml) under the guidance of a veterinary doctor. The general condition of the animals was observed, and they were euthanized with an overdose of pentobarbital if they showed cachexia. To the control quality, all the imaging examination, histology specimens obtained and the results of analyses were evaluated by the same physicians, but they do not know whether the animals received radiotherapy.

Radiotherapy process

Animals were placed in a prone position on a five-point fixation mask (Posicast Thermoplastics, Civco Medical Solutions, Kalowa, IA,USA) (Figure 2A). A Big Bore CT simulation scan (Brilliance Big Bore; Philips, Best, Netherlands) was used to defined the scanning area from the pelvis to the knee and marked with lead wire (Figure 2B).The contrast agent, iopamidol (Shanghai Bracco Sine Pharmaceutical Co. Ltd., Shanghai, China), was used in the dose of 2 ml/kg. The image was delivered to Eclipse treatment planning system (version 10.0, Varian Medical Systems, USA) to make it convenient for the physician

to delineate the target volume. The areas where tumor was located adjacent to the bones were defined as GTV_{boost} (gross tumor volume boost) and given the highest dose of radiation; GTV (gross tumor volume) included all tumors. CTV (clinical target volume) was defined as a 0.3–0.5 cm expansion of GTV on X-axis and Z-axis and a 3cm expansion on Y-axis. PTV (planning target volume) was defined as a 0.3–0.5 cm expansion of CTV (Figure 2C).

The prescription dose and radiotherapy plan was developed by Professor Jin-Rong Zhang and advanced physics engineer, Hao Liu, of the bone and STS multidisciplinary treatment study team. The conventional fractionation (CF) total dose of preoperative radiotherapy in STS is 50 Gy in 25 fractions of 2 Gy. The SIB schedule planned to a dose of 40 Gy, 35 Gy, 30 Gy, and 25 Gy was delivered to the GTV_{boost}, GTV, CTV, PTV respectively in 10 fractions (one fraction per day) over a planned course of 14days (2 weeks). Animals were not treated on weekends. The α/β ratio of tumor was set at 10 [15], so that the SIB schedule is close to the biological equivalent dose of CF, as shown in the following formula [16]:

$$n_2 d_2 \left(1 + \frac{d_2}{(\alpha/\beta)} \right) = n_1 d_1 \left(1 + \frac{d_1}{(\alpha/\beta)} \right)$$

$$\frac{D_2}{D_1} = \frac{1 + \dfrac{d_1}{(\alpha/\beta)}}{1 + \dfrac{d_2}{(\alpha/\beta)}}$$

$$BED = nd \times \left[1 + d/(\alpha/\beta) \right]$$

$$(SIB) 10 \times 4 \times \frac{14}{10} = 56 \prec 25 \times 2 \times \frac{12}{10} = 60 (CF)$$

Optimization and dose calculation was performed using the Eclipse treatment planning system with 6 MV photon beams from Varian Clinac IX linear accelerator (RapidArc™, Varian Medical Systems, Palo Alto, CA, USA) with the Millennium 120-mutileaf collimator. The Anisotropic Analytical Algorithm photon dosage calculation algorithm was used with a calculation grid set to 2.5 mm. Two full arcs were designed for VMAT radiotherapy (Figure 2D), with the rack rotating around the radiation field to form a coplanar radiation. After the completion of the plan, calibration was required before the implementation of radiotherapy (Figure 2E).

MR imaging

MRI was performed using a Magnetom Verio 3.0 T clinical MR scanner (Siemens, Healthcare Sector, Erlangen, Germany). Animals were placed in a prone position, and the tumors on their left hind limb were scanned using 3T Body MATRIX (TIM TRIO, Siemens Medical Solutions, Erlangen, Germany) assay.

The MRI sequence included 3D position, axial TSE T1WI, and TSE-FS T2WI. Scanning variables for T1WI were set as follows: TR=550 ms, TE=25 ms, FOV=200×200 mm², slice thickness=3.0 mm, averages=2. The variables for T2WI were set as follows: TR=4000 ms, TE=81 ms, FOV=200×200 mm², slice thickness=3.0 mm, averages=2.

DWI variables for sequence EP2D-DIFF were set as follows: TR=7400 ms, TE=79 ms, FOV=300×300 mm², slice thickness=3.0 mm, averages=5. Based on our pre-experiment, when the b-value was set at 600 s/mm², high-quality images could be obtained with lesion details, weighted diffusion, and high signal-to-noise ratio (SNR). Images were loaded onto a post-processing workstation (Syngo MMWP, Siemens Medical Solutions, Forchheim, Germany) for DWI and apparent diffusion coefficient (ADC) analyses, used to measure axial tumor diameter in each TSE-FS T2WI anatomic image. At those slice positions corresponding to the maximal axial diameter of each tumor, region-of-interest (ROI) measurements were performed. ROI for mean ADC measurements were drawn in GTV_{boost} area of the two groups. The ROI with a size ranging from 19 to 22 mm² underwent further quantitative analysis.

3D-PDA examination

A LOGIQ E9 Expert (GE Healthcare, Milwaukee, WI, USA) equipped with a multi-frequency probe (7–12 MHz,) that had been disinfected was placed parallel to the long axis of the rabbit femur, and 3D imaging was performed using Muscle-mode. Power Doppler images for the axial, sagittal, and coronal sections of the lesions were acquired and saved. The 3D-PDA semi-quantitative analysis of the volume data was performed using the manual mode of the Virtual Organ Computer-aided Analysis (VOCAL)-imaging program and the 15-rotation step. The 3D blood flow was imaged by delineating the tumor margin adjacent to the bones with plane A as the reference plane. According to their distribution and direction, tumor blood vessels were classified as type I: with dot- or line-like vessels around tumor but no vessel distribution in tumor, type II: with dot- or line-like vessels (simple branches, relatively straight) around and in the tumor, and type III: with rich vascular network (complex branches, tortuous pathways) in the tumor and visible vessels in tumor periphery [17].

Histological preparation

Two groups of animals were sacrificed under pentobarbital euthanasia, and tumors were resected very close to the bone. The areas, where tumor was located adjacent to the bone, were marked with a suture to assess the radiation at GTV_{boost} area made by SIB. The tumor was sliced at 3-mm intervals in the axial plane to correspond to the plane of the MR images, and was then fixed in 10% buffered formaldehyde solution. These samples
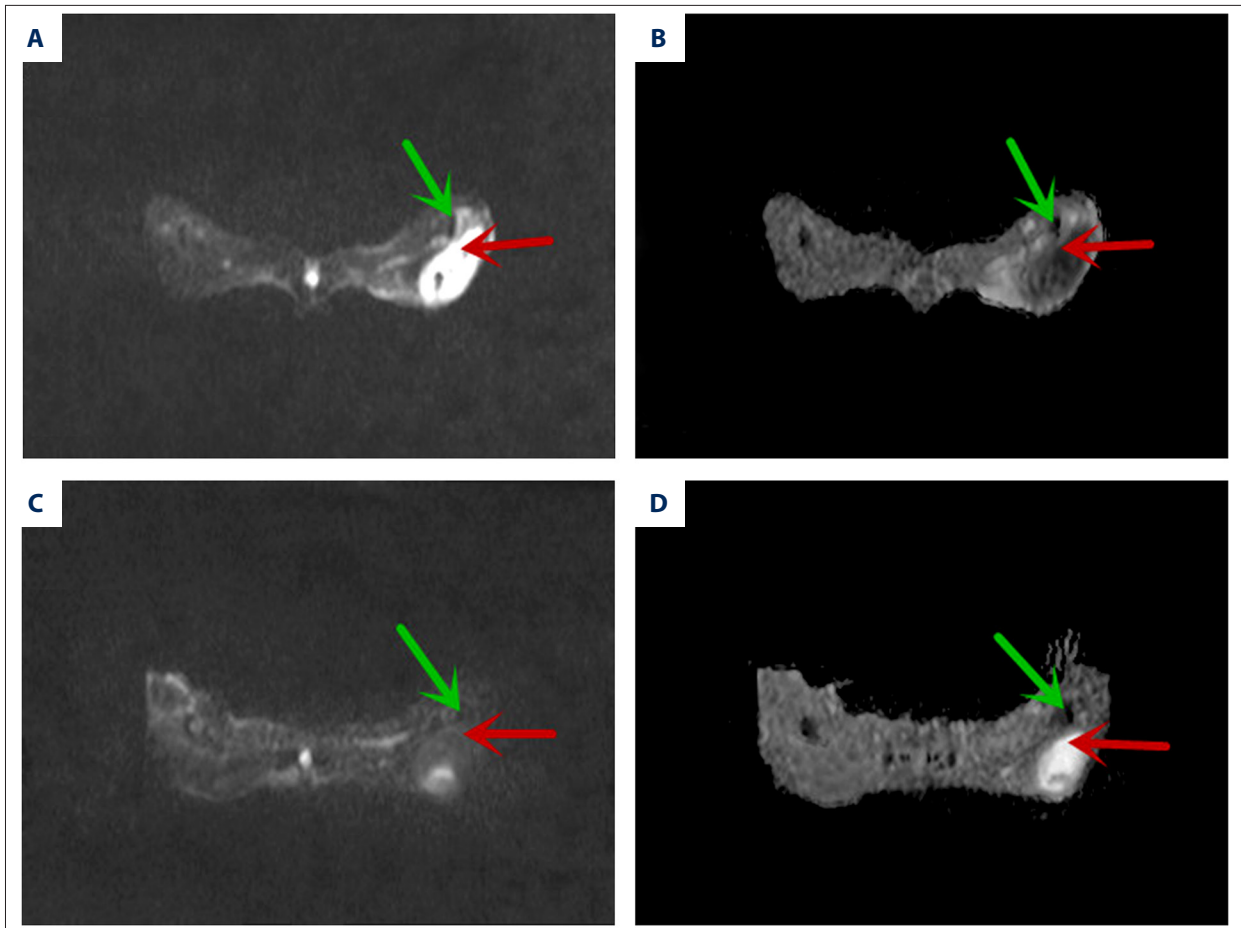
Figure 3. Signal intensity of GTV$_{boost}$ area in DWI and ADC maps after radiotherapy. In the control group, the GTV$_{boost}$ area showed a significantly high signal in DWI (**A**) and low signal in ADC maps (**B**). For the test group, the GTV$_{boost}$ area showed a significantly low signal in DWI (**C**) and high signal in ADC maps (**D**). Green arrow: femur. Red arrow: GTV$_{boost}$ area (areas where tumor was located adjacent to the bone).

were then sliced into 4-μm thick sections and stained using hematoxylin and eosin (HE) for tissue structure observation.

Statistical analysis

Statistical analysis was performed using SPSS 20.0 software, and measurement data were presented as mean ±SD. The variation of ADC value after radiotherapy was analyzed in a clustered bar and examined by unpaired two-tailed Student *t*-test. The comparison of 3D-PDA grades was made by Wilcoxon rank sum test and the test level α=0.05. Statistical significance was defined at $P \leq 0.05$.

Results

Animal models

B-ultrasound examination confirmed the successful establishment of VX2 limb tumor in 20 rabbits before radiotherapy.

No animal observed the local skin toxicity (radiation dermatitis) during that phase of the radiotherapy, and all the animals completed the radiotherapy protocol. Thus, 20 rabbits were eligible for the analysis.

MR Imaging

The DWI and ADC maps of the two groups showed a significant difference in the GTV$_{boost}$ area. Tumor necrosis was depicted as a region of low signal intensity on DWI, indicating free diffusion of water molecules, whereas viable tumor was depicted as a region of relative high signal intensity, indicating limited diffusion. The ADC maps displayed signal intensity opposite to that of DWI. The ADC value in necrotic area was significantly higher than the viable tumor because tumor cells had high density, intact cell membrane and restricted water diffusion, while the necrotic area had damaged cell membrane and unrestricted water diffusion.
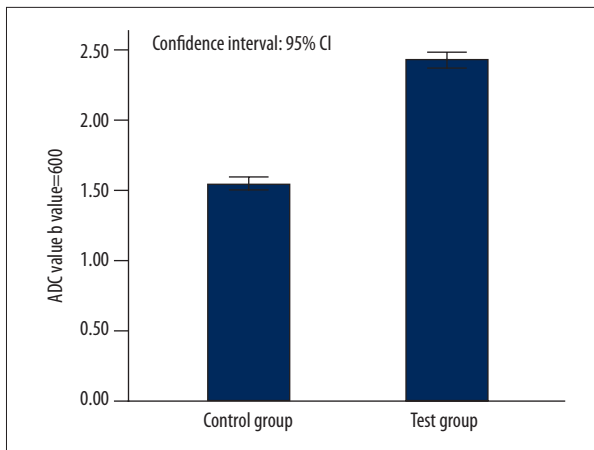
Figure 4. Clustered bar of ADC value change after radiotherapy in the GTV$_{boost}$ area. The ADC value of GTV$_{boost}$ area in the test group was significantly higher than that in the control (t=−28.83, P<0.05).

The control group displayed relatively long signal on axial T1WI and showed heterogeneous high signal on axial T2WI. The GTV$_{boost}$ area showed a significantly high signal in DWI (Figure 3A) and low signal in ADC maps (Figure 3B). The test group displayed relatively high signal on axial T1WI and showed a significantly high signal on T2WI. The GTV$_{boost}$ area showed a significantly low signal in DWI (Figure 3C) and high signal in ADC maps (Figure 3D).The ADC value of test group($2.41\pm0.09\times10^{-3}$ mm^2/s) was significantly higher than control group ($1.55\pm0.06\times10^{-3}$ mm^2/s) (Figure 4).

Table 1. 3D-PDA-based vessel classification.

Group	After radiotherapy		
	I	II	III
Control (10)	0	2	8
Test (10)	9	1	0

Wilcoxon rank sum test for independent samples showed that the vessel grades in the test group was significantly less than that in the control group after radiotherapy (Z=−4.03, P<0.05).

3D-PDA

The 3D-PDA analysis detected significant difference between the control and the test groups, as significantly decreased vascularization was observed at the GTV$_{boost}$ area in the test group. Based on the criteria of blood vessel classification, 2 and 8 vessels in the control group were classified as type II and type III vessels, respectively (Table 1). The control group displayed some vessel network with tortuous pathways inside the tumor, and peripheral thick vessels were observed (Figure 5A). In the test group, however, 9 vessels were classified as type I and only one was classified as type II. Tumor vascular structures decreased significantly, as no vessel distribution was detected in the tumor, and only dot- and line-like vessels were observed around the tumor (Figure 5B).
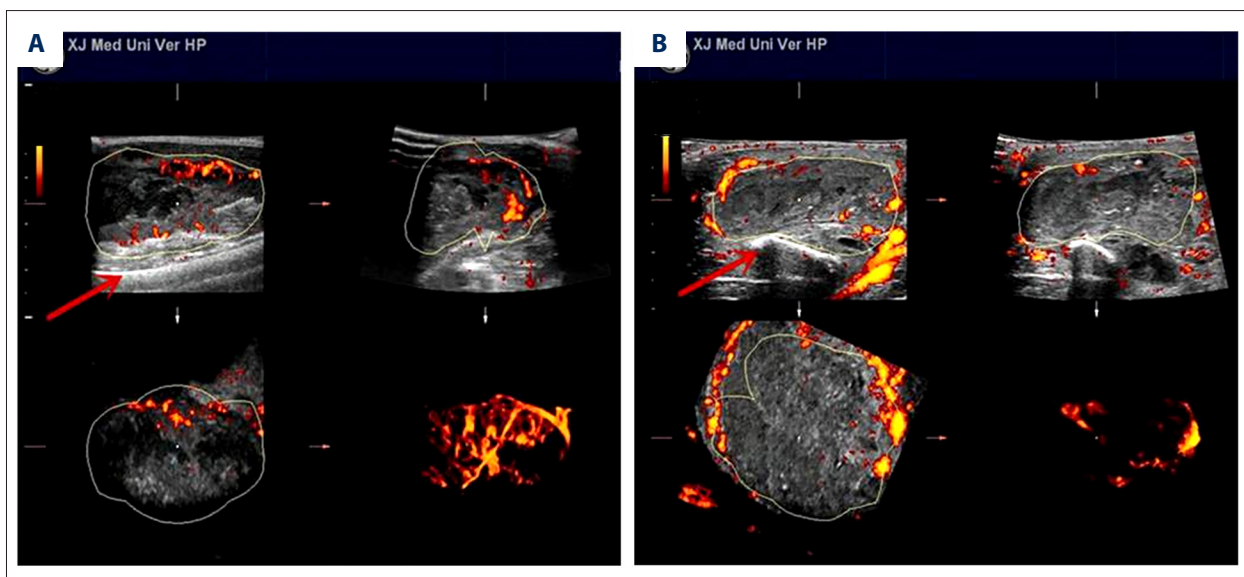

Figure 5. 3D-PDA images of two groups after radiotherapy. The control group displayed some vessel network with tortuous pathways inside the tumor, and peripheral thick vessels were observed (**A**). In the test group, tumor vascular structures decreased significantly, and only dot- and line-like vessels were observed around the tumor (**B**). Red arrow: femur.
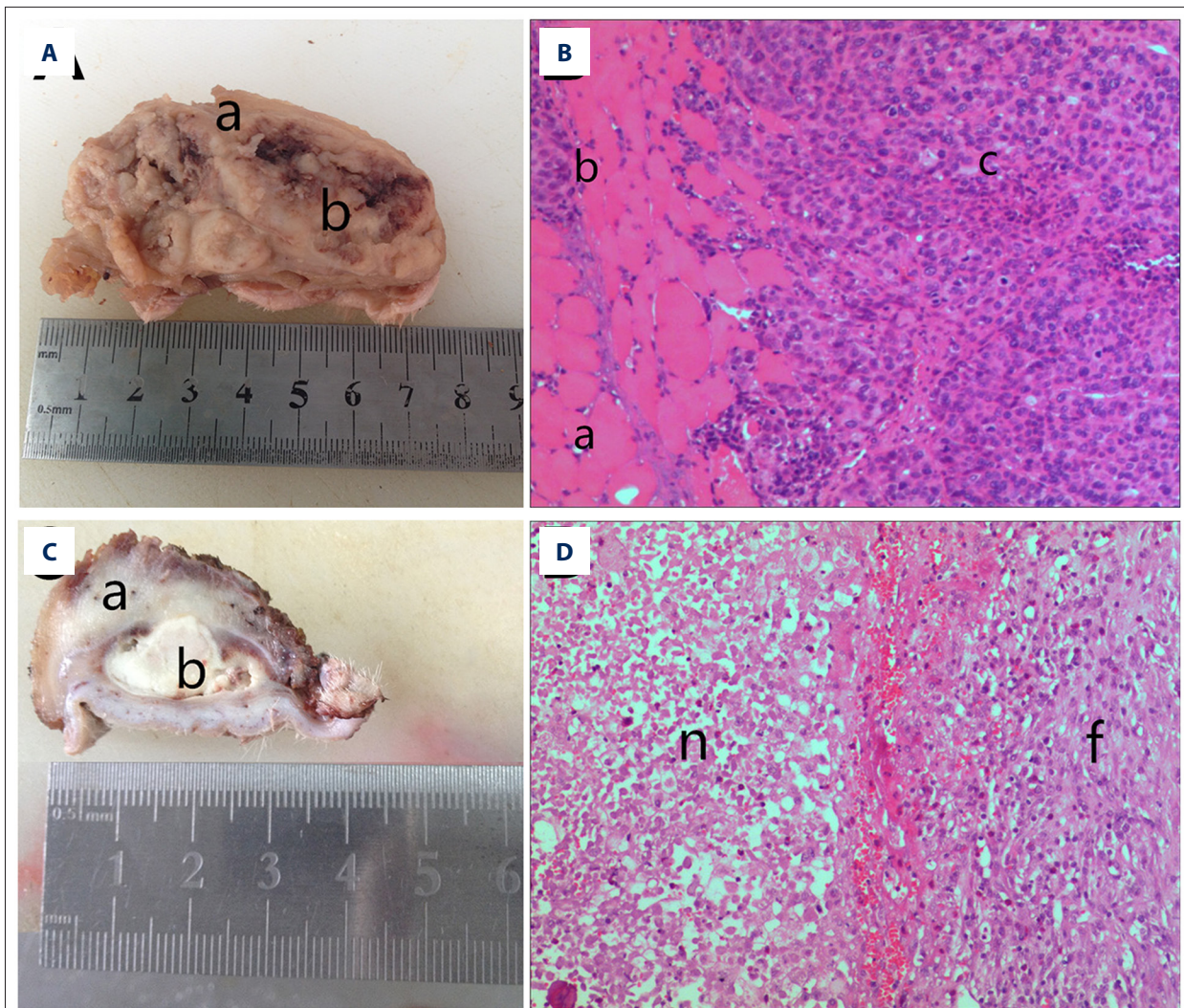
Figure 6. Histological changes after radiotherapy at GTV_{boost} area. In the control group, (**A**) a: tumor invasion of striated muscles, b: tumor tissues. (**B**) a: healthy muscle tissue, b: tumor invasion of striated muscles, c: tumor cells (×100). In the test group, (**C**) a: necrotic zone, b: tumor parenchyma necrosis, (**D**) n: large areas of necrosis, unclear cells boundaries with the surrounding tissues, f: fibroplasia (×100).

Histological analysis

Gross examination revealed the tumor parenchyma in the control group showing liquefaction necrosis, and fish meat-like tumor tissues were observed in GTV_{boost} area (Figure 6A). Observation of HE-staining under a 100× microscope showed that the tumor invasion of the striated muscles and normal structure of cells was damaged, and cell boundaries with surrounding tissues were unclear. In addition, tumor cells showed different sizes with increased cell density, enlarged and intensely stained nuclei, and some cells showed pathological mitosis (Figure 6B). In the test group, Gross examination showed that when the tumor specimens were cut transversely, GTV_{boost} area has a necrotic zone formation (Figure 6C). The tumor parenchyma showed a great deal of fluid and tofukasu-like tissue

spilled. Observation of HE-staining under a 100× microscope showed large areas of necrosis, unclear cell boundaries with the surrounding tissues, acute and chronic inflammatory cell infiltration, as well as fibroplasia in the necrotic zone (Figure 6D).

Discussion

To our knowledge, this is the first study that demonstrated the feasibility of using VMAT-SIB technique in the rabbit VX2 limb tumor model. No animal died during that phase of the radiotherapy. After radiotherapy, significant tumor necrosis was detected by MRDWI, and the GTV_{boost} area showed low signal in DWI and high signal in ADC maps. 3D-PDA observation showed that tumor vascular structures decreased significantly.

Histologic analysis demonstrated that a necrotic zone could be generated in the GTV$_{boost}$ area. Necrotic zone can be effectively defined as safe margin. Thus, in animal experiments, our hypothesis was initially confirmed.

Rabbit VX2 tumor model is a commonly used tumor model, it widely used in the oncologic study of image diagnosis and catheter-directed therapy [18–22]. In the pre-experiment, we found its biological behavior close to STS, as the tumor displays locally infiltrative growth and late pulmonary metastases. To establish the tumor model, we conducted B-ultrasound-guided tumor implantation to inject the tumor adjacent to the bone, thereby simulating biological behaviors of high-grade limb STS. In addition, many experimental studies of rabbit VX2 tumor model have demonstrated that tumors grew remarkably over 14th to 28th days after implantation [23]. So we initiated radiotherapy intervention after 2 weeks of implantation.

In the clinic, conventional preoperative radiotherapy cannot be accurate radiation for some high-grade limb STS with tumor adjacent to NVB or bones, and more complications occur after radiotherapy. Application of intensity modulated radiotherapy (IMRT) helps to improve target coverage and to spare critical structures better. However, IMRT plans and quality assurance requirements are more complex and time-consuming [11]. The VMAT showed a general improvement in sparing of organs at risk and healthy tissue, comparable target coverage, reduced beam-on time and lower number of monitor units (MU) compared with other IMRT approaches [12]. The SIB technique offers the possibility of reducing the number of fraction required, thus reducing the complexity and time of treatment delivery [13]. Scorsetti et al. reported that the 3-week course of postoperative radiation using VMAT with SIB showed to be feasible and was associated with acceptable acute skin toxicity profilein breast cancer patients [12].In this study, we performed pre-operative radiotherapy in the rabbit VX2 limb tumor model using VMAT-SIB, and enhanced local injury by increasing the radiation dose at GTV$_{boost}$ area. After that, a necrotic zone was generated. Gross examination observed the tumor tissues necrosis in the GTV$_{boost}$ area. Microscopic examination showed no tumor cells, but large areas of necrosis and the inflammatory cell infiltration and fibroplasia at the GTV$_{boost}$ area. Therefore, we were able to define the necrotic zone as "safe margin". Based on these findings, we suggest that in clinical practices, VMAT-SIB could be used for STS patients with tumor adjacent to NVB or bone. After radiotherapy, surgical resection of the tumor and operating within a safe margin increased the likelihood of wide resection, thereby reducing the local recurrence rate.

MRDWI can differentiate viable and necrotic tumor by reflecting the structure of the micro-environment and water molecules movement inside tumor. LIU et al. reported that DWI is a valuable tool for monitoring the response to radiotherapy of human prostate cancer [24]. Qian et al., Deng et al. and Geschwind et al. found that ADC value in necrotic tumor tissues were significantly greater than those in surrounding viable tumor tissues in the rabbit VX2 liver tumor model [18,21,22]. In the present study, since we did not inject a contrast agent, conventional MRI sequence at GTV$_{boost}$ area could not distinguish viable or necrotic tumor so that two groups displayed high signal intensity on axial T2WI after radiotherapy. However, the DWI and ADC maps detected areas of tumor necrosis, and especially, the ADC value was significantly increased in necrotic areas after radiotherapy. Compared with other studies [21,22], this study observed higher ADC value because tumor necrosis occurred in the muscles and water is abundant in the muscle tissues.

Alcazar et al. reported that 3D-PDA ultrasound is a relatively new and promising tool for a noninvasive assessment of tumor vascularization in gynecological malignancies [25]. In the present study, we did not use tumor volume to evaluate treatment response, but implemented semi-quantitative analysis to assess vessel changes in the tumor adjacent to the bones. Huang et al. found that cervical tumors and their vascularization disappeared within 3 months after radiotherapy [26]. Based on our pre-experiment, animals cannot tolerate conventional fractionation radiotherapy (total dose over a planned course of 5 weeks). In this study, we increase the prescription dose to reduce the number of fractionation. Thus, the test group revealed that tumor vascular structures decreased significantly, and only dot- and line-like vessels were observed around the tumor. In the clinic, most malignant tumor grow more slowly than VX2 rabbit tumor, and it takes long time for apoptosis and necrosis proceeding. Thus, histologic revealed the tumor parenchyma in the control group showing liquefaction necrosis. This could explain the control group displayed some vessel network with tortuous pathways inside the tumor. However, some limitations of 3D-PDA measurements exist, such as the size of the scan angle, which does not always allow acquisition of the whole tissue [27].

Histological analysis is critical to assess tumor response after radiotherapy. Ishii et al. found at 24 hours after radiotherapy, the number of viable tumor cells was markedly decreased, and the residual viable tumor cells showed nuclear condensation and nuclear collapse [14]. But this study of radiation dose is higher. In this study, our results revealed the DWI and 3D-PDA were detected, tumor necrosis and vascular structures were significantly decreased in the GTV boost area. However, histological examination further helped to identify the necrotic zone. Especially microscopic examination showed no tumor cells, but large areas of necrosis and the inflammatory cell infiltration and fibroplasia at the GTV$_{boost}$ area. Hence, histological analysis confirmed the effectiveness of safe margin

This work is licensed under a Creative Commons
Attribution-NonCommercial-NoDerivs 3.0 Unported License

2404

Indexed in: [Current Contents/Clinical Medicine] [SCI Expanded] [ISI Alerting System]
[ISI Journals Master List] [Index Medicus/MEDLINE] [EMBASE/Excerpta Medica]
[Chemical Abstracts/CAS] [Index Copernicus]

preparation. From a radiobiological perspective, the muscles belong to the late reactive tissue [28]. Thus, we conducted histological examination at 7 days after radiotherapy. Since radiotherapy continued for 2 weeks, and tumor necrosis might occur during each radiation, our study demonstrated earlier appearance of fibroblast compared with other studies [19].

The purpose of the present study was to assess the feasibility and effectiveness of preoperative radiotherapy using VMAT-SIB in preparing safe margin in the rabbit VX2 limb tumor model. But there are still some gap between the experimental design and clinical application. One of the limitations of our study is that we only performed short-term observation of the general status of animals at the end of radiotherapy; we failed to observe dynamic pathological changes after the necrotic zone formation. Another limitation is that we did not observe late local skin toxicity due to the shorter follow-up time. Further studies are needed to investigate dynamic

pathological changes of safe margin and local skin toxicity in the rabbit VX2 limb tumor model.

Conclusions

This study demonstrated that it is feasible to perform preoperative VMAT- SIB radiotherapy in the rabbit VX2 limb tumor model; by imaging and histological analysis, we confirmed that tumor tissues necrosis with adjacent bone after the implementation of VMAT-SIB, and the formation of necrotic zone can be effectively defined as safe margin. These findings provide an experimental basis for future clinical application.

Conflicts of interest

No additional external funding was received for this study. No competing financial interests exist.

References:

1. Kandel R, Coakley N, Werier J et al: Surgical margins and handling of soft-tissue sarcoma in extremities: a clinical practice guideline. Curr Oncol, 2013; 20(3): e247–54
2. Clark MA, Fisher C, Judson I, Thomas JM: Soft-tissue sarcomas in adults. N Engl J Med, 2005; 353(7): 701–11
3. Qureshi YA, Huddy JR, Miller JD et al: Unplanned excision of soft tissue sarcoma results in increased rates of local recurrence despite full further oncological treatment. Ann Surg Oncol, 2012; 19(3): 871–77
4. Potter BK, Hwang PF, Forsberg JA et al: Impact of margin status and local recurrence on soft-tissue sarcoma outcomes. J Bone Joint Surg Am, 2013; 95(20): e151
5. Kosela-Paterczyk H, Szacht M, Morysinski T et al: Preoperative hypofractionated radiotherapy in the treatment of localized soft tissue sarcomas. Eur J Surg Oncol, 2014; 40(12): 1641–47
6. Beane JD, Yang JC, White D et al: Efficacy of adjuvant radiation therapy in the treatment of soft tissue sarcoma of the extremity: 20-year follow-up of a randomized prospective trial. Ann Surg Oncol, 2014; 21(8): 2484–89
7. Soyfer V, Corn BW, Kollender Y et al: Hypofractionated adjuvant radiation therapy of soft-tissue sarcoma achieves excellent results in elderly patients. Br J Radiol, 2013; 86(1028): 20130258
8. O'Sullivan B, Davis AM, Turcotte R et al: Preoperative versus postoperative radiotherapy in soft-tissue sarcoma of the limbs: a randomised trial. Lancet, 2002; 359(9325): 2235–41
9. Sampath S, Schultheiss TE, Hitchcock YJ et al: Preoperative versus postoperative radiotherapy in soft-tissue sarcoma: multi-institutional analysis of 821 patients. Int J Radiat Oncol Biol Phys, 2011; 81(2): 498–505
10. Alongi F, Fogliata A, Navarria P et al: Moderate hypofractionation and simultaneous integrated boost with volumetric modulated arc therapy (RapidArc) for prostate cancer. Report of feasibility and acute toxicity. Strahlenther Onkol, 2012; 188(11): 990–96
11. Doornaert P, Verbakel WF, Bieker M et al: RapidArc planning and delivery in patients with locally advanced head-and-neck cancer undergoing chemoradiotherapy. Int J Radiat Oncol Biol Phys, 2011; 79(2): 429–35
12. Scorsetti M, Alongi F, Fogliata A et al: Phase I-II study of hypofractionated simultaneous integrated boost using volumetric modulated arc therapy for adjuvant radiation therapy in breast cancer patients: a report of feasibility and early toxicity results in the first 50 treatments. Radiat Oncol, 2012; 7: 145
13. Sladowska A, Hetnal M, Dymek P et al: Application of IMRT in adjuvant treatment of soft tissue sarcomas of the thigh-Preliminary results. Rep Pract Oncol Radiother, 2011; 16(3): 110–14
14. Ishii K, Hosono MN, Wada Y et al: Usefulness of FDG-microPET for early evaluation of therapeutic effects on VX2 rabbit carcinoma. Ann Nucl Med, 2006; 20(2): 123–30
15. Williams MV, Denekamp J, Fowler JF: A review of alpha/beta ratios for experimental tumors: implications for clinical studies of altered fractionation. Int J Radiat Oncol Biol Phys, 1985; 11(1): 87–96
16. Kuperman VY, Spradlin GS: Effect of variable dose rate on biologically effective dose. Int J Radiat Biol, 2013; 89(11): 889–97
17. Ohishi H, Hirai T, Yamada R et al: Three-dimensional power Doppler sonography of tumor vascularity. J Ultrasound Med, 1998; 17(10): 619–22
18. Qian T, Chen M, Gao F et al: Diffusion-weighted magnetic resonance imaging to evaluate microvascular density after transarterial embolization ablation in a rabbit VX2 liver tumor model. Magn Reson Imaging, 2014; 32(8): 1052–57
19. Wijlemans JW, Deckers R, van den Bosch MA et al: Evolution of the ablation region after magnetic resonance-guided high-intensity focused ultrasound ablation in a Vx2 tumor model. Invest Radiol, 2013; 48(6): 381–86
20. Yang RM, Zou Y, Huang DP et al: In vivo assessment of the vascular disrupting effect of M410 by DCE-MRI biomarker in a rabbit model of liver tumor. Oncol Rep, 2014; 32(2): 709–15
21. Deng J, Rhee TK, Sato KT et al: In vivo diffusion-weighted imaging of liver tumor necrosis in the VX2 rabbit model at 1.5 Tesla. Invest Radiol, 2006; 41(4): 410–14
22. Geschwind JF, Artemov D, Abraham S et al: Chemoembolization of liver tumor in a rabbit model: assessment of tumor cell death with diffusion-weighted MR imaging and histologic analysis. J Vasc Interv Radiol, 2000; 11(10): 1245–55
23. Larson AC, Rhee TK, Deng J et al: Comparison between intravenous and intraarterial contrast injections for dynamic 3D MRI of liver tumors in the VX2 rabbit model. J Magn Reson Imaging, 2006; 24(1): 242–47
24. Liu L, Wu N, Ouyang H et al: Diffusion-weighted MRI in early assessment of tumour response to radiotherapy in high-risk prostate cancer. Br J Radiol, 2014; 87(1043): 20140359
25. Alcazar JL, Jurado M, Lopez-Garcia G: Tumor vascularization in cervical cancer by 3-dimensional power Doppler angiography: correlation with tumor characteristics. Int J Gynecol Cancer, 2010; 20(3): 393–97
26. Huang YF, Cheng YM, Wu YP et al: Three-dimensional power Doppler ultrasound in cervical carcinoma: monitoring treatment response to radiotherapy. Ultrasound Obstet Gynecol, 2013; 42(1): 84–92
27. Galvan R, Merce L, Jurado M et al: Three-dimensional power Doppler angiography in endometrial cancer: correlation with tumor characteristics. Ultrasound Obstet Gynecol, 2010; 35(6): 723–29
28. Stewart FA, Akleyev AV, Hauer-Jensen M et al: ICRP publication 118: ICRP statement on tissue reactions and early and late effects of radiation in normal tissues and organs – threshold doses for tissue reactions in a radiation protection context. Ann ICRP, 2012; 41(1–2): 1–322